Materials Research Bulletin 51 (2014) 85–91

Contents lists available at ScienceDirect

Materials Research Bulletin

journal homepage: www.elsevier.com/locate/matresbu

Synthesis of silica coated zinc oxide–poly(ethylene-co-acrylic acid) matrix and its UV shielding evaluation

Mohankandhasamy Ramasamy [a,1], Yu Jun Kim [b,1], Haiyan Gao [b], Dong Kee Yi [c,*], Jeong Ho An [b,**]

[a] Division of Bionanotechnology, Gachon University, Seongnam 461-701, Republic of Korea
[b] Department of Polymer Engineering, Sungkyunkwan University, Suwon 440-746, Republic of Korea
[c] Department of Chemistry, Myongji University, Yongin 449-728, Republic of Korea

ARTICLE INFO

Article history:
Received 17 September 2013
Received in revised form 28 November 2013
Accepted 1 December 2013
Available online 6 December 2013

Keywords:
A. Nanostructures
B. Chemical synthesis
C. Photoelectron spectroscopy
C. Electron microscopy
D. Catalytic properties

ABSTRACT

Silica coated zinc oxide nanoparticles (Si-ZnO NPs) (7 nm thick) were synthesized successfully and melt blended with poly(ethylene-co-acrylic acid) (PEAA resin) to improving ultraviolet (UV) shielding of zinc oxide nanoparticles (ZnO NPs). The photostability of both the ZnO NPs and Si-ZnO NPs were analyzed by the difference in photoluminescence (PL) and by methylene blue (MB) degradation. Photo-degradation studies confirmed that Si-ZnO NPs are highly photostable compared to ZnO NPs. The melt blended matrices were characterized by field emission scanning electron microscopy interfaced with energy dispersive X-ray spectroscopy (FE-SEM-EDX). The UV shielding property was analyzed from the transmittance spectra of UV–visible (UV–vis) spectroscopy. The results confirmed fine dispersion of thick Si-ZnO NPs in the entire resin matrix. Moreover, the Si-ZnO/PEAA showed about 97% UV shielding properties than the ZnO/PEAA.

1. Introduction

Super-fine zinc oxide particles on the nanometer scale with high transparency work as a shield against a broad range of UV wavelengths. Being an inorganic material, ZnO has distinguished functions in the opto-electronics, photonics and textile industries. The semi-conducting nature, high surface to volume ratio, and high UV absorption make nanosized ZnO suitable for solar cells [1], light-emitting diodes [2], conducting films [3], catalysts [4,5], gas sensors [6], photo-luminescent devices [7], anti-microbial agents [8,9], wound dressings [10], cell labeling [11], and UV protection in cosmetics [12]. On the other hand, due to the high surface energy and large surface area, ZnO NPs tend to aggregate easily. Therefore, the surface of bare ZnO needs to be modified for a better dispersion. At the same time, the photocatalytic activity of the ZnO NPs must be reduced to make them safer UV absorbers and also the dispersability in aqueous media needs to be improved. Silica-based coatings are of particular interest because of their low refractive index, water-compatibility, lower toxicity and ease of surface functionalization [13].

There has been an increasing level of ultraviolet light radiation on the Earth's surface due to the global warming and other factors [14]. UV rays have harmful effect on human skin. Polymers, such as high-performance fabrics, lose strength and deteriorate after undergoing photodegradation by UV radiation upon long time exposure [15]. The high energy UV rays produce free radicals by homolytic bond cleavage and thus degrade and depolymerize polymers rapidly. Polymer degradation can be prevented by blending it with the proper UV absorbing materials. These agents can act in two ways: by quenching free radical produced and by reflecting, dispersing or absorbing high energies of UV radiation. The polymers and fabrics can be protected by filling with ZnO nanoparticles as UV protectors to make them more photo resistant. Zhao et al. reported that the polymer–nanoparticle melt blended extrudes show significant reduction in photodegradation [16]. Based on this, for the first time we made an attempt to produce efficient light shielding matrix for Nylon4 based fabrics, using PEAA resin as an interfacial agent and Si-ZnO as fillers.

Nanoparticle-embedded polymer matrices that shield UV rays but absorb visible light were formulated by using twin-screw extruder. Then photoluminescence, photodegradation, morphology (FE-SEM-EDX), acid dissolution and UV shielding activities were investigated.

* Corresponding author. Tel.: +82 31 330 6178.
** Corresponding author. Tel.: +82 31 290 7284.
E-mail addresses: vitalis@mju.ac.kr (D.K. Yi), jhahn1us@skku.edu (J.H. An).
[1] These authors contributed equally to this work.

0025-5408/$ – see front matter © 2013 Elsevier Ltd. All rights reserved.
http://dx.doi.org/10.1016/j.materresbull.2013.12.004

2. Experimental

2.1. Materials

ZnO solution (30 wt% in ethanol, Advanced Nano Particles Co., Ltd.), tetraethyl orthosilicate (TEOS, 99.999%, Sigma–Aldrich, USA), ethanol (99.9%, Samchun Chemicals, Korea), ammonium hydroxide (NH_4OH, 25–28%, DC Chemical, Korea), acetic acid (99.5%, Samchun Chemicals, Korea), poly(ethylene-co-acrylic acid) (PEAA resin, Dow Chemical Co., Ltd.), methylene blue (0.05 wt% solution in water, Sigma–Aldrich, USA) were used as received. In house Milli-Q water was used throughout the experiments.

2.2. Synthesis of silica coated ZnO NPs (Si-ZnO NPs)

The Si-ZnO NP hybrid was synthesized using a slight modification of the sol–gel process reported elsewhere [17]. Briefly, 35 ml of ethanol, 15 ml of water and 10 ml of NH_4OH (pH 12) were poured into a 100 ml round bottom flask with vigorous stirring. 0.5 g of ZnO dispersion and the appropriate amount of TEOS (30 wt% and 80 wt% to the amount of ZnO) were injected into the reaction flask. After 10 min of the ultrasonic treatment, this colloidal dispersion was stirred overnight for complete hydrolysis of TEOS [18]. The solid contents were collected by centrifugation at 5000 rpm (Sigma, 2-16PK), washed subsequently with ethanol three times, and then dried overnight in a vacuum oven at 60 °C. The thin and thick silica coating was achieved by adjusting the TEOS to ZnO weight ratio to 30 wt% and 80 wt%, respectively. Pure ZnO NPs were labeled as bare ZnO NPs.

2.3. Melt blending of poly(ethylene-co-acrylic acid) with ZnO NPs

The acrylic acid contents of the used PEAA resin were approximately 20 wt%. The ZnO and Si-ZnO NPs content in the matrix were set at 3 wt%. For comparison purpose, samples of unfilled PEAA processed under similar blending conditions were used. PEAA resin pellets and powder of bare ZnO and thick Si-ZnO NPs were dry-blended first. They were then melt blended and extruded using a twin-screw extruder (Bautek Co., ba-11) at 180 °C with a screw velocity of 200 rpm. These pellets were made to form a film with a thickness of 1 mm using a press machine (Sejin Technology Co., Ltd.) at 180 °C and 600 kg/cm^2. The sample was cut by liquid nitrogen and used for further analysis.

2.4. Characterizations

Nanoparticles were characterized by Fourier transform infrared (FT-IR) spectroscopy (Bruker, IFS-66/S) for its chemical modifications, UV–vis spectroscopy (Varian Inc., Cary 5000) and fluorescence spectroscopy (Varian Inc., Cary Eclipse) for its photostability studies, zeta potential measurements (Malvern Zeta-Sizer 3000HS) for its electrokinetic analysis at pH 7, and high resolution-transmission electron microscopy interfaced with energy dispersive X-ray spectroscopy (HR-TEM-EDX) (Tecnai G2 TF 30ST) for its morphology changes. The nanoparticle/PEAA matrices were characterized further for morphology studies and photoshielding abilities by FE-SEM-EDX (JEOL Corp., JSM6700F) and UV–vis transmittance spectroscopy, respectively.

2.5. Photostability

2.5.1. Study on PL intensity

The degree of photodegradation was assessed indirectly by measuring the change in PL intensity using a spectrofluorometer (Varian Cary Eclipse). Bare ZnO, thin Si-ZnO and thick Si-ZnO NPs were exposed to the UV light (CN-6 UV lamp, 60 Hz with 365 nm) for a maximum of 72 h, and the respective PL intensity response was recorded every 4 h.

2.5.2. Photodegradation measurement of MB

The photocatalysts (ZnO NPs) were dispersed into a MB aqueous solution and stirred for 30 min in the dark environment to achieve complete physical adsorption equilibrium. Subsequently, the reaction mixture was irradiated with UV light at a maximum of 180 min for the photodegradation study. At regular intervals, the samples were then taken from the reaction vessel and centrifuged quickly to avoid particle interference. The supernatant was measured by UV–vis spectroscopy at 664.1 nm and the resulting absorbance was measured and plotted as a function of time. The degree of MB degradation was calculated using the following equation [19]:

$$\text{Remaining MB}\,(\%) = (A_0 - A/A_0) \times 100\%$$

A_0 = initial absorbance, A = variable absorbance.

2.6. Study on dissolution

2.6.1. In acetic acid solution

Aqueous acetic acid at different concentrations was used as an acid solution medium. In 100 ml of pure water, acetic acid was added along with bare ZnO and thick Si-ZnO NP suspensions, separately. After stirring for 30 min, the samples were analyzed by UV–vis spectroscopy.

2.7. UV shielding effect

The UV-shielding properties of the nanoparticles and nanoparticle incorporated PEAA were compared by measuring the transmittance spectra of the corresponding films. The melt blended nanoparticle/PEAA matrices were cut into thin films at required sizes and further analyzed by FE-SEM-EDX and UV–vis spectrophotometer.

3. Results and discussion

Fig. 1 presents schematic view of the silica coating processes. The ZnO NPs were coated with silica by TEOS through hydrolysis and subsequent condensation in the presence of NH_4OH. In this sol–gel method, TEOS acts as a precursor and NH_4OH act as the catalyst. In the basic medium, the surface of the ZnO NPs was coated with OH layer. When TEOS was added to the solvent–nanoparticle mixture, the silane material began to undergo hydrolysis to establish ZnO–Si–OH linkage on the nanoparticle surface. In addition, a lateral polymerization reaction occurred with the excess silane material to form a three-dimensional siloxane bond (Si–O–Si) by leaving OH groups on the external surface. During the overnight aging, a tight homogeneous silica shell over the particles was formed.

Fig. 2 presents the FT-IR spectra of bare ZnO and Si-ZnO NPs. The peaks at 1550–1700 cm^{-1} and 3100–3600 cm^{-1} can be attributed to the hydroxyl groups of water. The Si–O–Si asymmetric stretching vibration band of 980–1190 cm^{-1} was found only in the Si-ZnO NPs spectrum compared to the bare ZnO NPs [20,21]. The Si-ZnO bond formation was confirmed by the reduction in peak intensity at 700–750 cm^{-1} of Si–O–Si. This manifests the existence of a silica layer and successfully grafted over the ZnO NPs.

The HR-TEM images (Fig. 3) of the bare ZnO, thin Si-ZnO, and thick Si-ZnO NPs showed the clear existence of a ZnO core with distinguishable silica shells (marked with arrows). A thin layer of the silica shell was observed in Fig. 3(B), 2 nm in size, which also

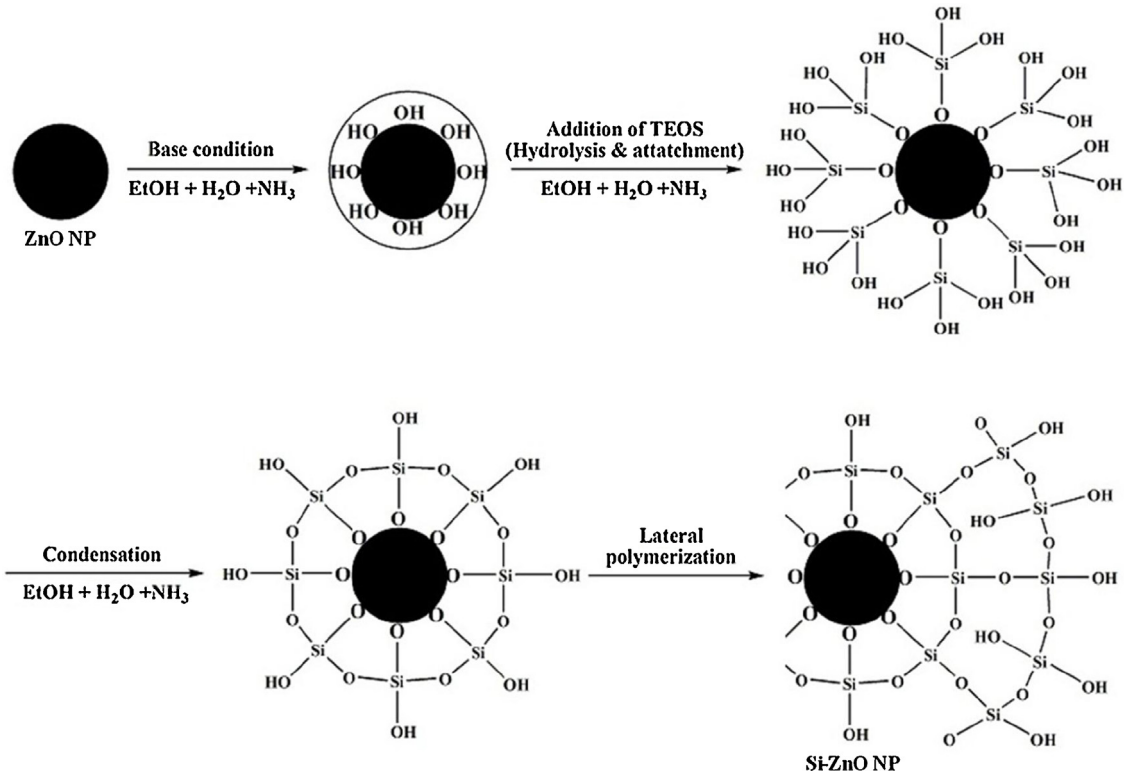

Fig. 1. Schematic diagram of the sol–gel chemistry involved in the silica coating of the ZnO nanoparticles.

shows an uneven covering over the core shell of the nanoparticles. Fig. 3(C) shows the formation of a thick, uniform silica layer, 7 nm in thickness, resulting from the high concentration of silane material. The silica layers formed over the ZnO NPs were verified further by the EDX and zeta potential measurements.

Fig. 3(D)–(F) presents the corresponding EDX spectra of the bare, thin and thick Si-ZnO NPs, reflecting the chemical composition of both the core and silica shell with Zn, O and Si. Furthermore, quantitative elemental analyses of the bare ZnO particles were compared with that of the surface modified particles and the results are listed in Table 1. From EDX analysis, 0.02 wt% of silica was observed in the thin Si-ZnO NPs, whereas in thick Si-ZnO NPs the same was 0.19 wt%. The increased Si content was responsible for the gained silica thickness from 2 nm to 7 nm. The quantity of the peak Si was enhanced (Fig. 3(E) and (F)), which is in good agreement with the TEM images (Fig. 3(B) and (C)).

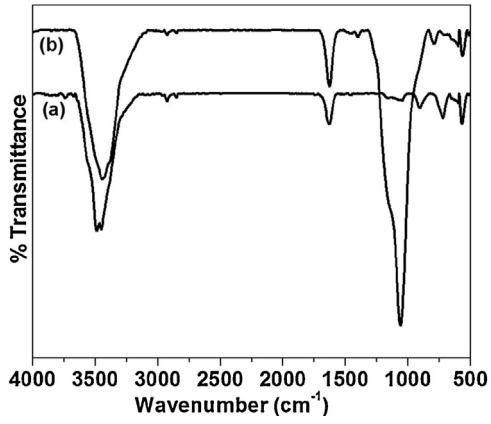

Fig. 2. FT-IR spectra of (a) bare ZnO NPs and (b) Si-ZnO NPs.

In zeta potential study the bare ZnO NPs showed a value of +31.0 mV. After modification, the charge reversal became −23.7 mV for the thin Si-ZnO particles and −43.6 mV for the thick Si-ZnO NPs. A high negative zeta potential of the thick Si-ZnO NP was attributed to the bulky silica layer with many Si–OH groups at the surface.

When light was illuminated on the semiconductor (ZnO) surface, which has photocatalytic activity, the electron–hole pair diffused out on the surface due to the weaker bond energy. This electron and hole interact with the surrounding oxygen or water to produce free radicals with strong oxidization capability, which degrades the organic compounds, such as dyes and polymers [22]. Furthermore, the photocorrosion of the semiconductor nanoparticles causes photoetching of the particles to reduce the size, increases the energy gap and allows agglomeration to form larger particles [23]. Considering these facts, the surface of nanoparticles was coated with silica to prevent the photocorrosion of ZnO NPs.

Fig. 4 presents the PL response of the nanoparticles after UV light irradiation. With time, the bare ZnO NPs showed less photostability toward light irradiation. Therefore, the PL decreases significantly to 80% in 72 h. In contrast, thick Si-ZnO NPs show only ca. 5% reduction in the entire exposure time. On the other hand, the thin Si-ZnO NPs showed a slow decrease of about 50% ZnO during the entire exposure time which is faster than thick Si-ZnO NPs. This might be due to the very thin silica shell or incomplete silica layer, which is insufficient to prevent photocorrosion. These results suggest strongly that, a thick silica shell over ZnO NPs either prevents the excited electrons from being involved in free radical generation or photoetching after monochromatic light exposure. Compared to the silica coated ZnO NPs, the uncoated particles were attacked easily by strong light due to photoetching to make it unstable [23]. Therefore, through high energy irradiation, the photostability of semiconducting nanoparticles was decreased due to an increase in surface defects in the form of an energy gap.

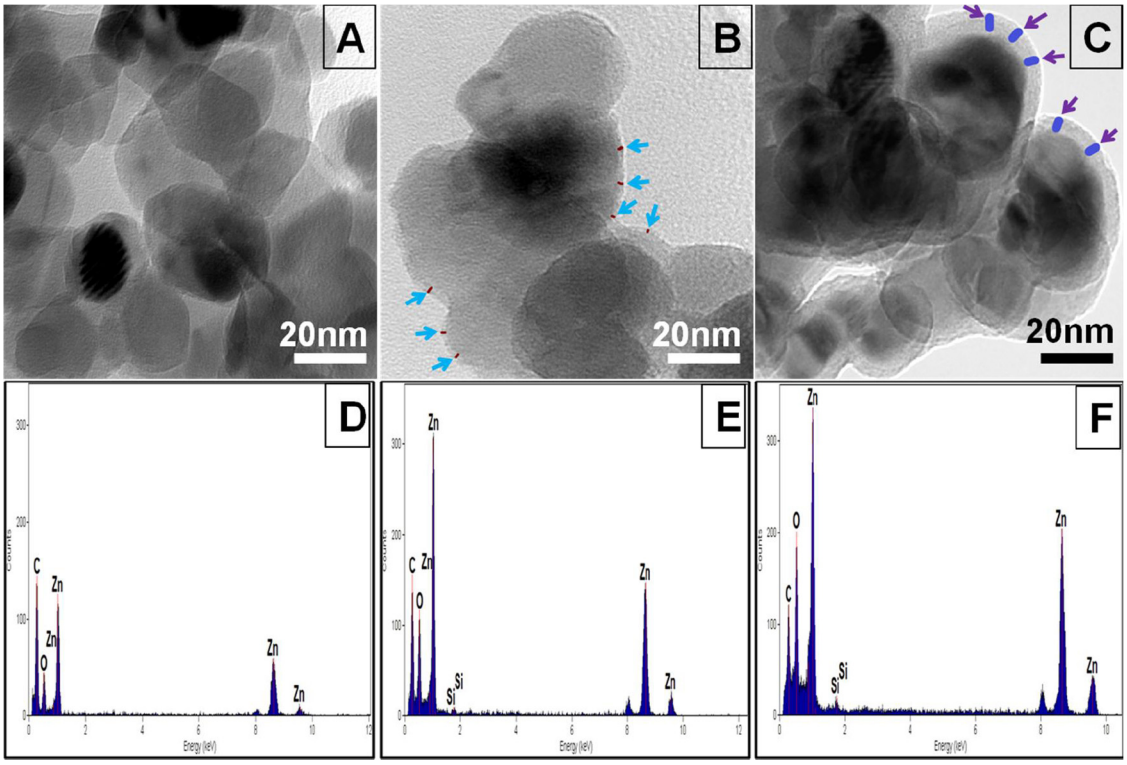

Fig. 3. HR-TEM images of (A) bare ZnO, (B) thin Si-ZnO, and (C) thick Si-ZnO NPs (arrows indicating silica shell) and their corresponding elemental spectrums as D, E and F.

In addition, the photodegradation behaviors of bare, thin and thick Si-ZnO NPs were assessed against an aqueous MB solution. Fig. 5 shows the relationship between the change in MB absorbance ($A_0 - A$) vs. irradiation time (t). The MB degradation of 55% and 12% was observed with the thin Si-ZnO and thick Si-ZnO NPs, respectively. These results suggest that silica coated nanoparticles show reduced photodegradation compared to the un-coated ZnO NPs, which is in good agreement with previously reported results [24]. The un-coated ZnO NP under UV irradiation caused either the migration of electrons/generated holes on the surface or oxygen active species formed, which decomposed the MB from blue to colorless in a quick manner. Thin Si-ZnO NPs improved the considerable photostability but the degradation was increased with increasing the UV irradiation time. This could be due to the non-uniform silica layer. When the TEOS to ZnO ratio was increased, the 7 nm thick silica shell was formed and affords protection to the ZnO surface to avoid contact with MB. The shielding effect of the SiO_2 layer that formed on the nanoparticles can be responsible for the inhibition of the photocatalytic activity. The electronic bands of SiO_2 are located far lower and higher in energy than the corresponding bands of ZnO. Therefore, the SiO_2 layer acts as a barrier to prevent the motion of electrons/holes generated in ZnO on the surface [25,26]. These results suggest that a thin silica shell would not provide better photostability, rather thick silica coated ZnO NPs showed strong inhibition of photodegradation by leaving ~95% of the MB unaffected, even after extended irradiation times. These results suggest Si-ZnO NP could be a better photostable agent to make highly photostable polymer matrix. Althues et al. [27] presented the UV absorption capabilities of pure ZnO and silicon added ZnO particles. They showed that the UV absorption significantly decreased with increasing silicon contents. But, our synthesized Si-ZnO NPs showed superior UV absorption as well as visible absorption functions with thick silica shell compared to the absorption of bare ZnO NPs. We achieved efficient UV absorption properties of ZnO with thick silica shell and hence it could be applied as a strong UV blocking agent.

Fig. 6 shows the UV–vis absorption spectra of the bare and Si-ZnO NPs. The concentration of nanoparticles was kept constant and their UV–vis absorption responses toward different acetic acid concentrations were measured (Table 2). The absorption peak at 370 nm was assigned to the characteristic band-gap peak of ZnO

Table 1
Percentage elemental composition of the bare, thin and thick Si-ZnO NPs from EDX analyses.

Sample	Bare ZnO NPs		Thin Si-ZnO NPs		Thick Si-ZnO NPs	
Element	Weight%	Atomic%	Weight%	Atomic%	Weight%	Atomic%
C (K)	41.81	65.56	19.32	40.12	40.87	65.55
O (K)	19.58	23.05	24.71	38.52	18.63	22.43
Si (K)	0.00	0.00	0.02	0.02	0.19	0.13
Zn (K)	38.61	11.38	55.93	21.33	40.29	11.87

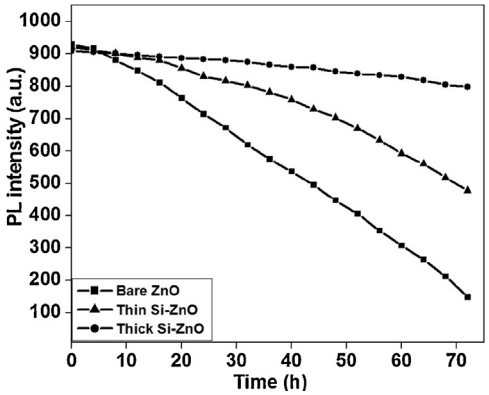

Fig. 4. Change in the photoluminescence intensity difference for nanoparticle suspensions under UV irradiation at different times.

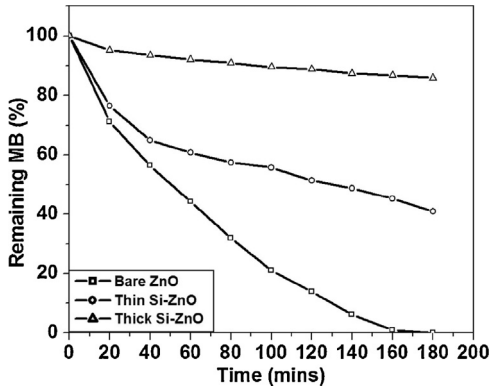

Fig. 5. Time-dependant degradation rate of methylene blue against UV irradiation on nanoparticles.

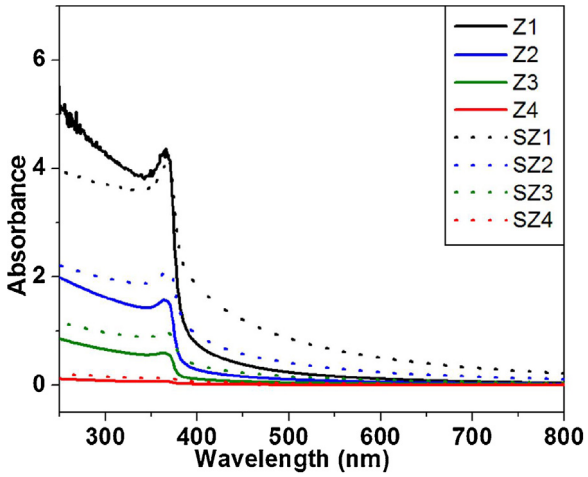

Fig. 6. UV–vis absorbance spectra of (Z1–Z4) bare and (SZ1–SZ4) thick Si-ZnO NPs in the aqueous acetic acid.

[28]. Initially, the absorbance intensity was higher without acetic acid (Z1 and SZ1) but the absorbance intensity of the bare ZnO NPs (Z2–Z4) decreased with increasing acetic acid concentration. This indicates the complete dissolution of ZnO by the acid. An aqueous solution of acetic acid might transform ZnO to the zinc acetate complex, which does not absorb UV light. The absorbance peak was not observed for the highest concentration of acetic acid used. Even the densely silica coated ZnO NPs (SZ2–SZ4) recorded a similar pattern of an absorption intensity reduction like the bare ZnO NPs. The silica coating on ZnO has many micro- and meso-pores, and these pores can work as direct openings for contacting acid with the ZnO surface [29]. An aqueous acetic acid at high concentration dissolves all the ZnO regardless of its surface coverage, either thick or thin silica layer.

In earlier studies the outdoor efficiency of ZnO was assessed by mixing it with a complex wood polymer lignin [30]. It was found that delamination from the wood surface was decreased after UV light and moisture exposure due to the presence of ZnO coating. It was concluded that ZnO coating with polymer showed enhanced photostability results which made them a preferred coating material for outdoor applications. Thus we applied the same hypotheses to make UV protective polymer matrix exclusively for outdoor use.

While for making the inorganic nanoparticle incorporated polymer fibers as UV blocking fabrics with Nylon4, we observed that, the ZnO completely melted and dissolved in the extruder. Hence, the PEAA resin is selected as an interfacial agent to embed with ZnO. But the acid groups present in the PEAA resin degrade

Table 2
Sample names, concentration of acetic acid and nanoparticles used in the dissolution study.

Sample code	Acetic acid	Bare ZnO NPs	Sample code	Acetic acid	Thick Si-ZnO NPs
Z1	None	0.002 mol (0.163 g)	SZ1	None	0.002 mol (0.203 g)
Z2	0.002 mol (0.120 g)	0.002 mol (0.163 g)	SZ2	0.002 mol (0.120 g)	0.002 mol (0.203 g)
Z3	0.003 mol (0.180 g)	0.002 mol (0.163 g)	SZ3	0.003 mol (0.180 g)	0.002 mol (0.203 g)
Z4	0.004 mol (0.240 g)	0.002 mol (0.163 g)	SZ4	0.004 mol (0.240 g)	0.002 mol (0.203 g)

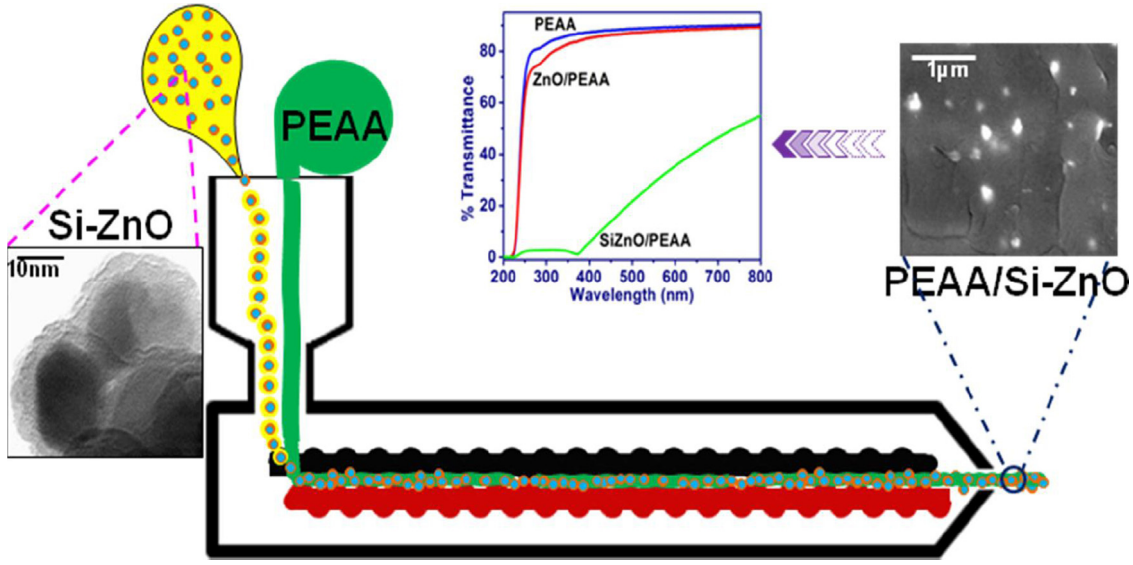

Fig. 7. Schematic drawing resembling the synthesis and characterization results of ZnO/PEAA polymer matrix.

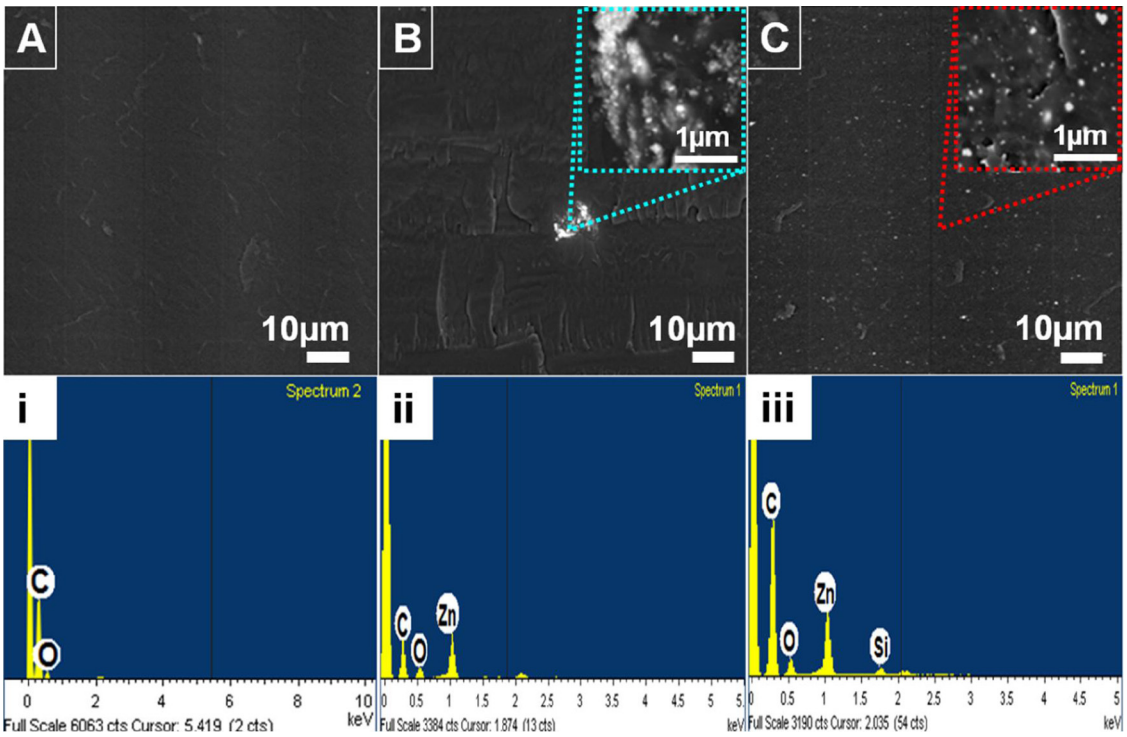

Fig. 8. FE-SEM images of (A) PEAA resin, (B) bare ZnO/PEAA, (C) thick Si-ZnO/PEAA (insets as magnified images) and their corresponding EDX spectra as (i), (ii), and (iii).

the ZnO to form ZnO-PEAA salt. Thus the ZnO are coated with silica and then combined with the PEAA resin to be used as a UV blocking polymer with Nylon4. Fig. 7 shows a schematic representation of the synthesis of Si-ZnO/PEAA matrix and its photoshielding abilities.

The ZnO NP content of 3 wt% was selected to PEAA resin as an optimum concentration. Because, no NP, or a lower or higher wt% NP used could damage the entire system upon UV irradiation and could cause undesirable results [16,31]. Images A, B, and C in Fig. 8 show FE-SEM images of the PEAA resin, bare ZnO NPs embedded PEAA (bare ZnO/PEAA), and thick Si-ZnO embedded PEAA (Si-ZnO/PEAA), respectively. A difference between each sample can be observed clearly because they are on the same scale. PEAA resin indicates the morphology of the plain, smooth surface without any particles. ZnO/PEAA shows the uneven attachment of bare ZnO NPs in the resin, which have been observed as agglomerates (inset). Fig. 8(C) and its magnified image show a highly uniform distribution of thick Si-ZnO NPs on the entire resin surface. This is easily distinguishable with the bright dots found on the resin surface due to the higher atomic weight nanoparticles by photon excitation. A complete high level dispersion of Si-ZnO resulted from the melt blending process to yield more efficient light shielding polymer matrix.

Here, the melt blended Si-ZnO were intercalated into the layers of PEAA resin. The OH groups and defective bonds of silica layer in Si-ZnO surface could form weak interaction with the carbonyl group of PEAA to form solid-metal complex, which shield the entry of aqueous acid. Basically, the silica particles are not disintegrated easily by weak acids like acrylic acid. But, the result of Fig. 6 shows that the Si-ZnO NP were completely disintegrated by acetic acid. This was due to the direct contact of acid to the ZnO surface through micro- and meso-pores present in the silica layer. In contrast, while melt blending of Si-ZnO NP with PEAA such pores were blocked thus ZnO could not come in direct contact with the acid groups of PEAA. Hence, Si-ZnO/PEAA showed stronger stability toward acid degradation as compare to bare ZnO/PEAA.

Fig. 8(i)–(iii) shows the EDX analyses results. The elemental spectrum confirmed the existence of Zn for the ZnO/PEAA matrix, Zn and Si for Si-ZnO/PEAA matrix and none for the PEAA resin (appearance of C and O derived from the supporting substrate).

Fig. 9(i) and (ii) shows the comparative UV–vis transmittance spectroscopy results of bare ZnO and Si-ZnO, before and after adding with PEAA resin. As compared to the other existing UV absorbers, our thick silica coated ZnO NPs showed the advantages of competitive UV shielding and high visible light transmittance ability, enhanced dispersion in PEAA resin, and protected the ZnO from acid group degradation.

Fig. 9(ii)(a) shows the PEAA resin with high transparency toward light. But, when the ZnO is mixed with PEAA resin there are minor differences in the visible-light transparency but improved UV-shielding ability was observed (Fig. 9 (ii)(b)). Approximately 4% of the UV rays were screened by the bare ZnO/PEAA matrix but 96% passed through the nanoparticle resin matrix, which may degrade the co-polymer structure of the PEAA resin. Even though the ZnO alone shows good UV shielding ability (from Fig. 9(i)(a)), when it is mixed with PEAA resin, the ZnO/PEAA matrix became transparent toward light. This might be due to the ZnO degradation by the acid groups in the PEAA resin. In contrast, thick Si-ZnO NPs with a higher silica content of 80 wt% engrafted in the PEAA resin showed a considerable UV shielding property of approximately 97% than the ZnO/PEAA matrix (Fig. 9(ii)(c)). At wavelengths smaller than 380 nm less transmission is observed. It could be attributed to the semiconductor nanocrystals (ZnO), where their absorption edge is energetically related to the band gap [27]. In the visible-light region, the Si-ZnO/PEAA matrix maintained a reduced transparency of approximately about 50% at 800 nm compared to the ZnO/PEAA matrix. This is based on the size of ZnO core, the larger NPs reducing the transparency of the matrix, while the smaller ZnO NPs in decreased amounts show better transparency with excellent UV shielding effect. As like Si-ZnO (from Fig. 9(i)(b)), the Si-ZnO/PEAA matrix also shows similar transmittance spectra revealing that the Si-ZnO even after attaching with PEAA resin still maintains

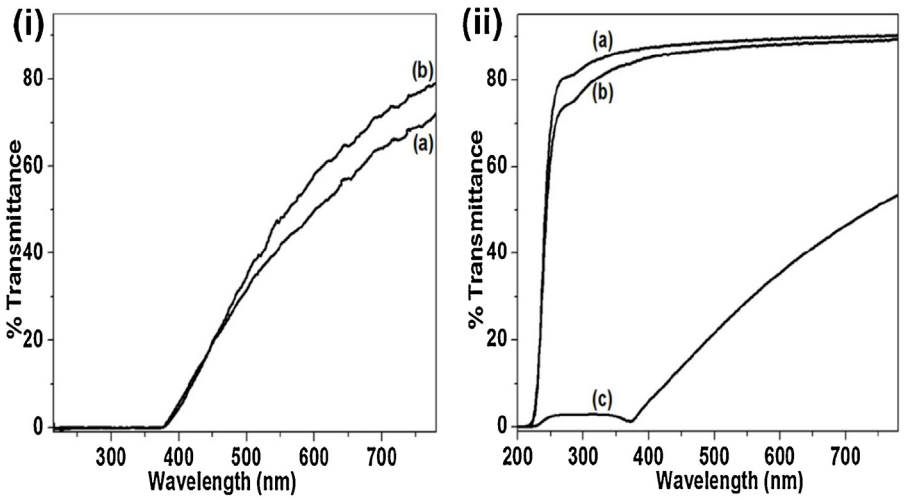

Fig. 9. UV–vis transmittance spectra of (i) (a) bare ZnO, (b) thick Si-ZnO and (ii) (a) PEAA resin, (b) bare ZnO/PEAA and (c) thick Si-ZnO/PEAA matrix.

satisfactory UV shielding property without causing any degradation to the polymer. This might be due to an increase in the silica layer thickness around the nanoparticles can hinder the acid dissolution of ZnO by the PEAA resin as well as the degradation of the PEAA resin by UV rays, which makes Si-ZnO/PEAA a better UV shielding matrix. Although this is an initial trial to control the silica thicknesses on ZnO NP for applying in polymer matrices, further studies will be made to optimize the parameters for effective applications.

4. Conclusions

Silica coated ZnO NPs were synthesized using a sol–gel process with a controllable thickness by adjusting the silane material to ZnO NPs concentration. HR-TEM showed that the ZnO NPs were coated with a continuous and uniform thick silica layer. In addition, EDX, zeta potential, and FT-IR confirmed the successful surface coating of silica over the ZnO NP. Further, PL study and MB degradation also support that the thick silica coating effectively stabilize ZnO from the light.

FE-SEM with EDX showed the successful formation of the Si-ZnO/PEAA matrix after a fine dispersion of Si-ZnO NPs in the PEAA resin matrix. The UV–vis transmittance spectra confirmed that the Si-ZnO/PEAA showed enhanced UV shielding ability and less visible-light transparency than the ZnO/PEAA matrix.

These results confirmed that the surface passivation over photocatalysis enhances their photostability toward a dye solution. Simultaneously, the formation of a nanoparticle-incorporated matrix with the PEAA resin by a melt blending process improves the UV shielding property and it could be used for making UV protecting fabrics with Nylon4.

Acknowledgment

This research was supported by the Industrial Strategic Development Program (10047657, development of platform technology for the synthesis of the structure controlled acrylic flow modifier) funded by the Ministry of Trade, Industry and Energy (MI, Korea).

References

[1] Q.B. Meng, K. Takahashi, X.T. Zhang, I. Sutanto, T.N. Rao, O. Sato, A. Fujishima, H. Watanabe, T. Nakamori, M. Uragami, Langmuir 19 (2003) 3572–3574.
[2] L.F. Dong, J. Jiao, D.W. Tuggle, J.M. Petty, S.A. Elliff, M. Coulter, Appl. Phys. Lett. 82 (2003) 1096–1098.
[3] A. Shimizu, S. Chaisistsak, T. Sugiyama, A. Yamada, M. Konagai, Thin Solid Films 361 (2000) 193–197.
[4] M.L. Curridal, R. Comparelli, P.D. Cozzli, G. Mascolo, A. Agostiano, Mater. Sci. Eng. C 23 (2003) 285–289.
[5] V.P. Kamat, R. Huehn, R. Nicolaescu, J. Phys. Chem. B 106 (2002) 788–794.
[6] T. Gao, T.H. Wang, Appl. Phys. A 80 (2005) 1451–1454.
[7] R.S. Yadav, P. Mishra, A.C. Pandey, Ultrason. Sonochem. 15 (2008) 563–868.
[8] N. Jones, B. Ray, K.T. Ranjit, A.C. Manna, FEMS Microbiol. Lett. 279 (2008) 71–76.
[9] G. Singh, E.M. Joyce, J. Beddow, T.J. Mason, J. Microbiol. Biotechnol. Food Sci. 2 (2012) 106–120.
[10] P.T. Kumar, V.K. Lakshmanan, R. Biswas, S.V. Nair, R. Jayakumar, J. Biomed. Nanotechnol. 8 (2012) 891–990.
[11] X. Tang, E.S. Choo, L. Li, J. Ding, J. Xue, Langmuir 25 (2009) 5271–5275.
[12] A.S. Dussert, E. Gooris, J. Hemmerle, Int. J. Cosmet. Sci. 19 (1997) 119–129.
[13] D.K. Yi, Mater. Lett. 65 (2011) 2319–2321.
[14] http://earthobservatory.nasa.gov/IOTD/view.php?id=79198 (23.04.13).
[15] J.W.S. Hearle, High Performance Fibers, CRC Press/Woodhead Publications, New York, 2002.
[16] H. Zhao, H.Y.R. Li, Polymer 47 (2006) 3207–3217.
[17] C.J. Brinker, G.W. Scherer, Sol–Gel Science, Academic Press, New York, 1990.
[18] A. Jaroenworaluck, W. Sunsaneeyamatha, N. Kosachan, R. Stevens, Surf. Interface Anal. 38 (2006) 473.
[19] R. Wang, J.H. Xin, Y. Yang, H. Liu, L. Xu, J. Hu, Appl. Surf. Sci. 227 (2004) 312–317.
[20] E. Liden, L. Beergstrom, M. Person, R. Carlsson, J. Eur. Ceram. Soc. 7 (1991) 361–368.
[21] I.A. Siddiquey, T. Furusawa, M. Sato, N. Suzuki, Mater. Res. Bull. 43 (2008) 3416–3424.
[22] J. Yao, C.X. Wang, Int. J. Photoenergy 643182 (2010) 1–6.
[23] T. Torimoto, J.P. Reyes, K. Iwasaki, B. Pal, T. Shibayama, K. Sugawara, H. Takahashi, B. Ohtani, J. Am. Chem. Soc. 125 (2003) 316–317.
[24] J. Zhai, X. Tao, Y. Pu, X.F. Zeng, J.F. Chen, Appl. Surf. Sci. 257 (2010) 393–397.
[25] E. Palomares, J.N. Clifford, S.A. Haque, T. Lutz, J.R. Durrant, J. Am. Chem. Soc. 125 (2003) 475–482.
[26] R.Y. Hong, T.T. Pan, J.Z. Qian, H.Z. Li, Chem. Eng. J. 119 (2006) 71–81.
[27] H. Althues, P. Potschke, G.M. Kim, S. Kaskel, J. Nanosci. Nanotechnol. 9 (2009) 2739–2745.
[28] A.K. Zak, M.E. Abrishami, W.H. Majid, R. Abd Yousefi, S.M. Hosseini, Ceram. Int. 37 (2011) 393–398.
[29] D.K. Yi, S.S. Lee, G.C. Papaefthymiou, J.Y. Ying, Chem. Mater. 18 (2006) 614–619.
[30] F. Weichelt, R. Emmler, R. Flyunt, E. Beyer, M.R. Buchmeiser, M. Beyer, Macromol. Mater. Eng. 295 (2010) 130–136.
[31] J. Lee, D. Bhattacharyya, A.J. Easteal, J.B. Metson, Curr. Appl. Phys. 8 (2008) 42–47.